JOURNAL OF
Materials
CHEMISTRY

A spectroscopic study of the effect of the trivalent cation on the thermal decomposition behaviour of Co-based hydrotalcites

J. Pérez-Ramírez,* G. Mul, F. Kapteijn and J. A. Moulijn

Industrial Catalysis, DelftChemTech, Delft University of Technology, Julianalaan 136, 2628 BL Delft, The Netherlands. Tel: 31 (0)15 278 4356; Fax: 31 (0)15 278 5006; E-mail: j.perezramirez@tnw.tudelft.nl

Received 5th June 2001, Accepted 8th August 2001
First published as an Advance Article on the web 6th September 2001

Various correlations between the size of the trivalent cation (Al, Ga, Fe, and Cr) and the structural characteristics and decomposition behavior of Co-based hydrotalcites ($Co/M^{3+} = 3$) have been identified. *In situ* IR spectra (by the relative ratio of the amount of carbonate in low and high symmetry) and thermogravimetric analyses show that the larger the trivalent cation, the lower the relative amount of water in the interlayer space of the as-synthesized material. Removal of interlayer water upon decomposition induces a symmetry loss of the carbonate groups, leading to splitting of the ν_3 vibrational mode of the carbonate groups at elevated temperatures. The extent of splitting was found to continuously decrease as a function of increasing cation size, which suggests a decreasing degree of interaction of the carbonate groups with remaining OH groups in the brucite-like layers. However, the stability of the carbonates in the temperature range of 200–250 °C shows an opposite trend, and is apparently dependent on other factors, such as the stability of the hydroxides and the layered structure itself, as well as direct interactions of carbonate with the metal ions. Dehydroxylation of the brucite-like layers, followed by complete carbonate decomposition are the final stages leading to the formation of mixed metal oxides.

1. Introduction

Synthetic hydrotalcite-like compounds (HTlcs) or layered double hydroxides (LDHs) have been subject of many studies: syntheses, preparations and structural studies, as well as applications as sorbents, anion exchangers, catalyst supports and catalyst precursors have been reported.[1,2] Hydrotalcites are hydrated hydroxycarbonates of lamellar structure with a general formula $[M^{2+}{}_{1-x}M^{3+}{}_x(OH)_2][A^{m-}]_{x/m}\cdot nH_2O$, and can be visualized as brucite-type octahedral layers, in which M^{3+} cations partially substitute for M^{2+} cations. The positive charge resulting from this substitution is balanced by anions (often carbonate) and water molecules arranged in interlayers alternating with the octahedral sheets.[3,4]

Upon thermal decomposition, HTlcs form homogeneously dispersed mixed oxides with a high surface area. The type of the cations in the layers, and of the anions in the interlayer can be changed, and thus many opportunities for fine tuning of the catalytic properties are available. The thermal decomposition mechanism of these materials is of crucial importance in catalysis, since the catalytic properties of the final mixed oxide largely depend on the activation procedure, *e.g.* in hydrogenation of acetonitrile over decomposed Ni–Al hydrotalcites or in N_2O decomposition over decomposed Co-based hydrotalcites.[5,6]

Kannan and Swamy[7] have previously investigated the effect of the trivalent cation (Al, Fe, Cr) on the physico-chemical properties of Co-containing anionic clays and the mixed oxides obtained by decomposition, but neither the application of *ex situ* techniques, nor the study of the as-synthesized material and the product after calcination at 400 °C for 5 h provides a detailed description of the thermal decomposition mechanism.

We have recently applied an integration of *in situ* techniques to describe the thermal decomposition mechanism of Co–Al-HTlc in different atmospheres, as well as the effect of the divalent cation on the thermal decomposition mechanism of Co–Al- and Ni–Al-HTlcs.[8–10] In this contribution we have extended the study of Kannan and Swamy[7] (including Ga in the series of trivalent cations) to temperatures between 25 and 550 °C using *in situ* FT-IR spectroscopy, and provide a more detailed assignment and description of the spectra at room temperature and during thermal decomposition. The spectroscopic results are interpreted using X-ray diffraction and thermogravimetric analyses. The results are used to derive conclusions on the effect of the trivalent cation on the thermal decomposition behaviour of Co-hydrotalcites.

2. Experimental

2.1. Material preparation

Co-hydrotalcites with different trivalent cations M^{3+} (Al, Ga, Fe, and Cr) were prepared by co-precipitation at constant pH and temperature at low supersaturation conditions, as previously described.[11] A flow ($2\ l\ h^{-1}$) of an aqueous solution of the respective metal nitrates $Co(NO_3)_2\cdot 6H_2O$ (>99.0%, Merck), $Al(NO_3)_3\cdot 9H_2O$ (>99.0%, Fluka), $Fe(NO_3)_3\cdot 9H_2O$ (>99.0%, Merck), $Ga(NO_3)_3\cdot 6H_2O$ (>99.0%, Fluka), and $Cr(NO_3)_3\cdot 9H_2O$ (>99.0%, Alfa) with a total cation concentration of 1.5 M was mixed slowly at 22 °C in the required metal molar ratios under vigorous agitation with an alkaline solution of Na_2CO_3–NaOH. The nominal molar Co/M^{3+} ratio was 3 in all the preparations. The carbonate concentration was adjusted to obtain a molar $CO_3{}^{2-}/M^{3+}$ ratio of 2. The pH of the precipitates was kept at 9.5, by adjusting the flow rate of the alkaline solution. After addition of the reactants the slurry was aged at 65 °C for 18 h under mild stirring. A reflux unit was mounted on top of the precipitation vessel to prevent water evaporation. Finally, the material was cooled to room temperature, filtered, washed with a large amount of warm (30 °C) deionized water, and dried at 90 °C for 12 h.

2.2. Material characterization

The chemical composition of the as-synthesized hydrotalcite-like materials was determined by Inductive Coupled

DOI: 10.1039/b104989p

Plasma-Optical Emission Spectroscopy (ICP-OES) (Perkin-Elmer 40 (Si) and Optima 3000DV (axial)).

X-Ray diffraction (XRD) patterns of the as-synthesized materials and the calcination products at 550 °C for 3 h were measured using a Bruker AXS diffractometer with Bragg–Brentano geometry, and Cu-Kα radiation (λ = 0.1541 nm). Data were collected in the 2θ range 5–75° with a step size of 0.1° 2θ and a counting time of 8 s. Determination of the cell parameters of the hydrotalcite (a and c) and the decomposed oxide (a) samples, was described in detail previously.[9,10] In all cases, the observed interplanar d spacing was corrected using elemental Si as an external standard (JCPDS 27-1402). The Scherrer equation was used to estimate the crystallite size of the as-synthesized and decomposed materials.

Thermal analysis (TGA–DSC) was carried out in a Thermal Sciences STA 1500H apparatus. The solid (10 mg sample with SiC dilution to a total weight of 50 mg, particle size 75–100 μm) was placed in alumina sample crucibles (70 μl) using α-Al_2O_3 as reference. Analyses were performed in a dry air flow of 100 cm^3 min^{-1} STP at atmospheric pressure. The temperature was increased from 25 to 1000 °C with a heating rate of 10 °C min^{-1}.

The *in situ* Fourier transform IR (FT-IR) spectra were recorded on a Nicolet Magna 550 Fourier transform spectrometer using a Spectratech diffuse reflectance (DRIFT) accessory, equipped with a high temperature cell. The transitions during thermal activation of 20 mg of hydrotalcite were studied *in situ* in air (25 cm^3 min^{-1} STP). The spectra were collected at room temperature and in the range 100–550 °C at intervals of 50 °C using a heating rate of 10 °C min^{-1}. The spectra were acquired by coaddition of 256 scans (approximate scanning time 300 s), with a nominal resolution of 4 cm^{-1}. KBr (Alfa, FTIR grade) was used to record the background.

3. Results and discussion

3.1. Chemical analysis

Elemental chemical analysis data indicate that the molar metal Co/M^{3+} ratio in the as-synthesized samples (between 2.8 and 3.1) was close to the value in the parent solutions (Co/M^{3+} = 3). This indicates that the precipitation step was carried out effectively.

3.2. X-Ray diffraction

The XRD patterns of the as-synthesized materials (not shown) were similar to those typically reported in the literature for layered double hydroxide materials.[1,7] Hydrotalcite (JCPDS 14-0191) was the only crystalline phase identified in the samples. Fig. 1 shows that the a parameter of the as-synthesized materials increases linearly with increasing size of the trivalent cation. The ionic radii of the cations used in this study were taken from ref. 1. The c parameter slightly decreases with increasing size of the trivalent cation, especially from Co–Ga-HTlc to Co–Fe-HTlc. This is related to the degree of hydration of the different samples and will be discussed in detail in sections 3.3 and 3.4.

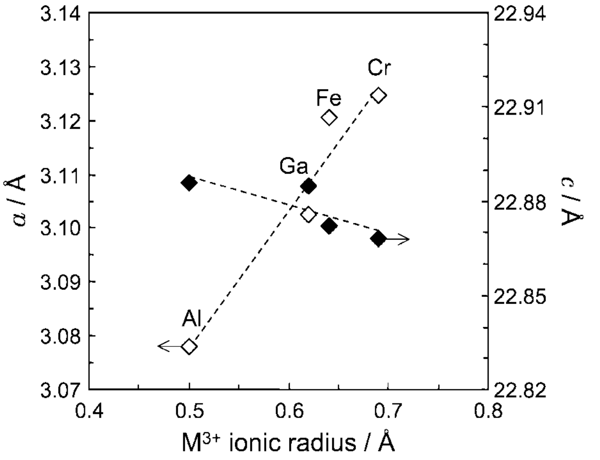

Fig. 1 Relation of the lattice parameters a and c of the as-synthesized Co-based hydrotalcites as a function of the ionic radius of the trivalent cation in the sample. Cell parameters calculated according to ref. 9.

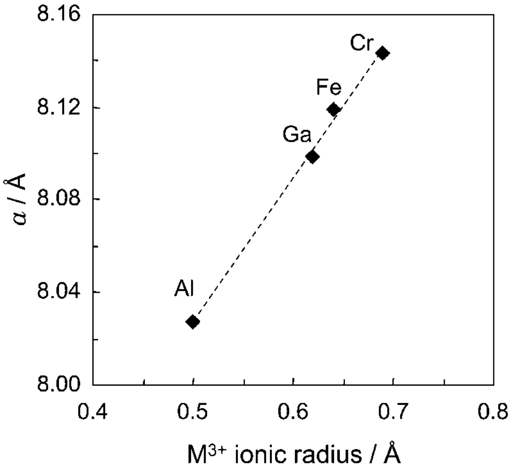

Fig. 2 Relation of the lattice parameter a of the Co-based mixed oxides as a function of the ionic radius of the trivalent cation in the sample. Cell parameters calculated according to ref. 9.

Thermal decomposition of Co–M^{3+}-HTlcs in air at 550 °C for 3 h leads to the formation of a cobalt spinel phase. Due to the similar reflection angles and intensities in XRD (not shown), it is not possible to distinguish between Co_3O_4, $CoM^{3+}{}_2O_4$, and $Co_2M^{3+}O_4$. Based on the molar Co/M^{3+} ratio of the as-synthesized materials, a solid solution of trivalent cations in Co_3O_4 is likely to be formed (denoted as $Co(M^{3+},Co)_2O_4$), as previously proposed for Co–Al-HTlc.[9,12] The a parameters of the Co-based mixed oxides show a linear correlation with the size of the trivalent cation in the (cubic) oxide structure (Fig. 2). The a values of these oxide samples are lower than the values reported for pure spinels, which also indicates the formation of non-stoichiometry, in the form of anion vacancies and/or dissolution of M^{3+} ions in the spinel phase.

The average crystal sizes ($\bar{D}$) of the as-synthesized materials and the corresponding mixed oxides are compared in Fig. 3. The values range from small crystallites of 4.5 mm in Co–Cr-HTlc

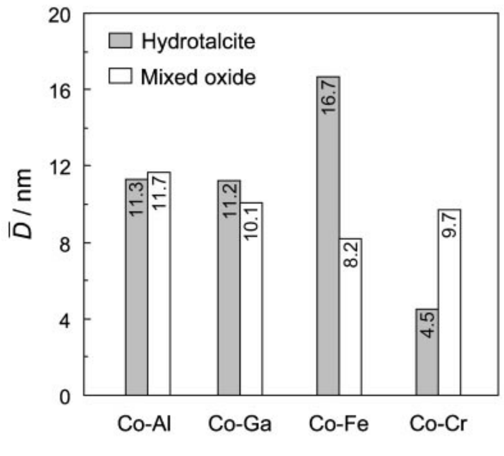

Fig. 3 Average crystal sizes $\bar{D}$ of the different as-synthesized Co-based hydrotalcites (solid bars) and their corresponding decomposition products at 550 °C for 3 h (open bars).

to large crystals of 16.7 nm in Co–Fe-HTlc. Intermediate crystallite sizes were found for Co–Al- and Co–Ga-HTlcs (11.3 and 11.2 nm, respectively). This suggests that the crystallinity of the co-precipitated material is strongly influenced by the nature of the trivalent cation, since the synthesis procedure was similar. Furthermore, decomposed Co–Al-HTlcs and Co–Ga-HTlcs show a very similar crystal size to that of the corresponding as-synthesized materials, suggesting that the morphology of the crystals in these samples did not change significantly upon heat treatment in air. However, the crystal size of the samples containing Fe diminishes considerably, while the crystallinity of the Co–Cr mixed oxide is enhanced with respect to that of the hydrotalcite. From this result it is concluded that the morphology of the crystals in the mixed oxides changes upon thermal decomposition depending on the trivalent cation in the formulation, but without a clear trend.

3.3. Thermal analysis

The TGA–DSC profiles of the thermal decomposition of the as-synthesized samples in air are shown in Fig. 4(a)–(d). Two relatively sharp endothermal transitions (I and II) can be identified in the DSC profiles, which is typical for layered materials.[13–15] The weight loss in transition I is usually related to the removal of water from the interlayer space and occurs in the range 135–200 °C. The peak temperature of transition I in the DSC profiles and the corresponding weight loss follow a trend with the size of the trivalent cation (Fig. 5(a)): the larger the cation the lower the weight loss and the lower the temperature for the occurrence of transition I. The different weight loss of the samples in transition I is attributed to the amount of water in the interlayer space, in agreement with the

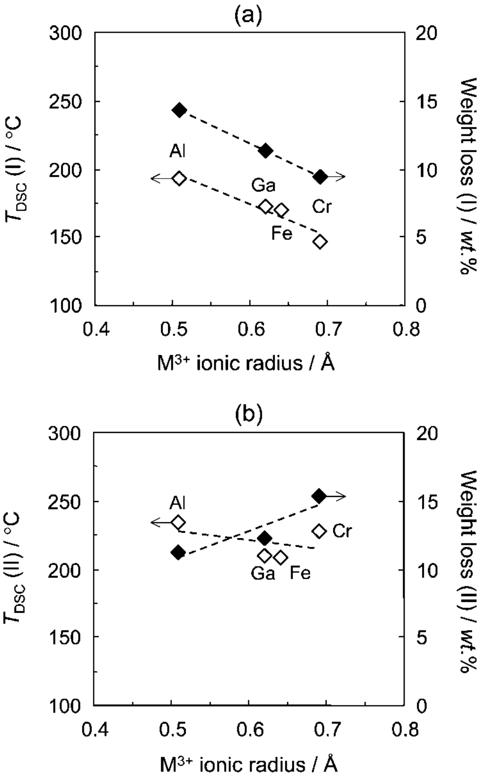

Fig. 5 Correlation of the (◆) weight loss and (◇) peak temperature with the ionic radius of the trivalent cation in the Co-based hydrotalcites during (a) transition I and (b) transition II from the TGA–DSC profiles in Fig. 4.

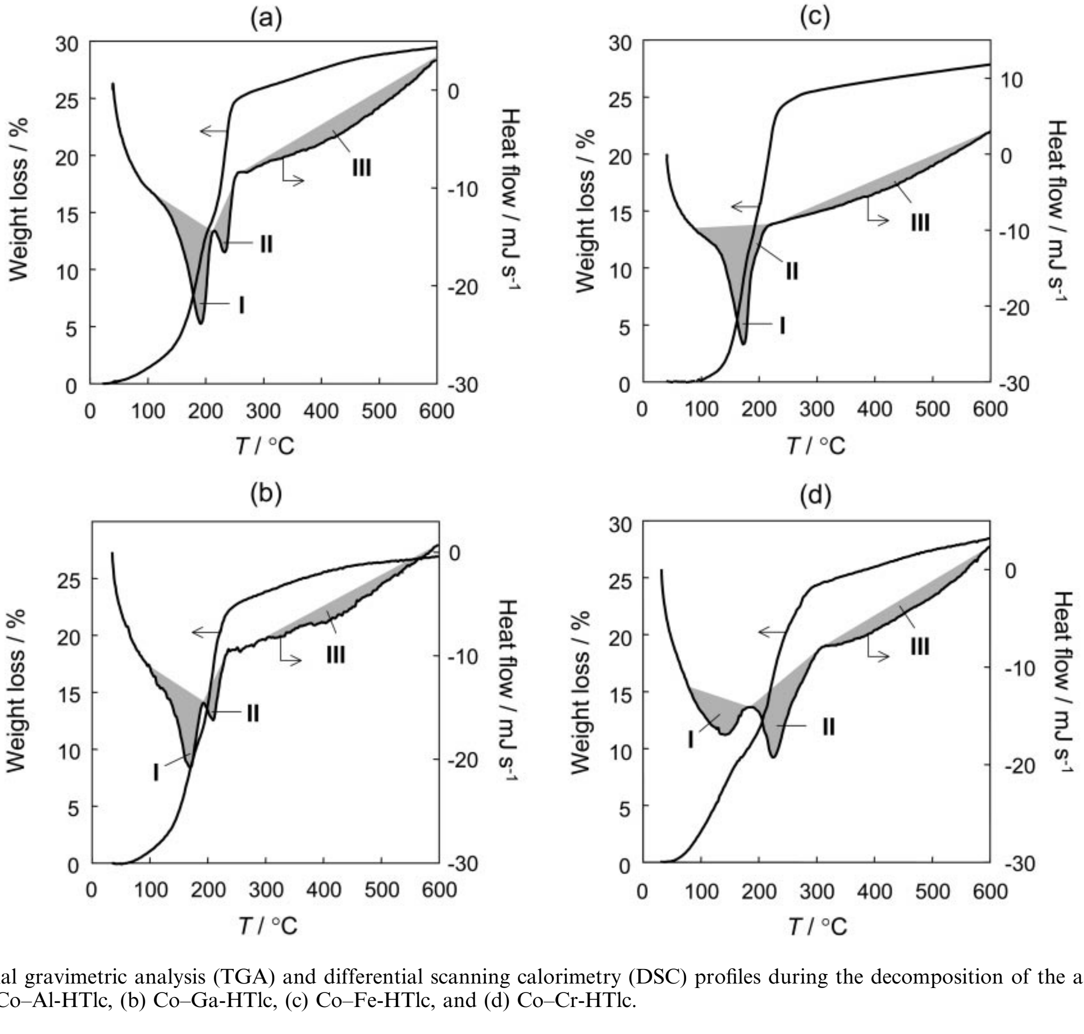

Fig. 4 Thermal gravimetric analysis (TGA) and differential scanning calorimetry (DSC) profiles during the decomposition of the as-synthesized samples: (a) Co–Al-HTlc, (b) Co–Ga-HTlc, (c) Co–Fe-HTlc, and (d) Co–Cr-HTlc.

trend observed for the *c* parameter in Fig. 1. In the correlation between weight loss and ionic radius, Co–Fe-HTlc was not included due to its particular thermal behaviour. The TGA and DSC profiles of this sample (Fig. 4(c)) show a simultaneous release of interlayer water, structural water, and CO_2 around 175 °C, with a small shoulder at 200 °C, leading to an apparent single step of weight loss. This pattern makes any discrimination impossible in terms of weight loss and/or thermal transitions of the different processes taking place during decomposition.

Transition II occurs in the temperature range 200–250 °C and is generally assigned to the complete dehydroxylation of the brucite-like sheet leading to the collapse of the layered structure and formation of the oxide phase. In this stage, partial decomposition of the carbonates also occurs. Peak temperatures for transition II in the different samples do not show a clear trend (Fig. 5(b)): Co–Cr-HTlc shows a relatively high peak temperature in the second transition, similar to that of Co–Al-HTlc. Kannan and Swamy[7] also observed the remarkably high stability of this material, the second transition leading to a decomposition temperature of about 300 °C. These authors attributed the anomalous behaviour of Co–Cr-HTlc to the poor crystallinity of the hydrotalcite phase, which is induced by the nature of the trivalent cation. The weight loss in transition II increases as a function of the cation size, but the correlation is not very clear (Fig. 5(b)). This is likely related to the simultaneous decomposition of both hydroxyl and carbonate groups[8,9] of which the relative contribution to the weight loss might vary as a function of the trivalent ion. Based on the weight loss *a priori* it is impossible to discriminate between decarbonation and dehydroxylation. The broad endothermal signal above 250 °C (shown as III in Fig. 4) is assigned to the removal of remaining carbonate groups in the decomposed material, as supported by *in situ* IR spectroscopy. This residual weight loss was very similar in all the samples ($\sim$5 wt.%) up to thermal decomposition at 600 °C.

3.4. *In situ* FT-IR spectroscopy

IR spectra recorded at room temperature, as well as during the decomposition in air of the Co-based hydrotalcites with different trivalent cations in the temperature range 25–550 °C are shown in Fig. 6(a)–(d). The various assignments and physico-chemical transformations described below are summarized in Table 1 and Scheme 1.

3.4.1. As-synthesized hydrotalcites. *Water and hydroxyl vibrations.* In the IR spectra of Co-based hydrotalcites at room temperature, broad adsorption bands at 3500–3545 cm^{-1} and 3050 cm^{-1} (shoulder) are observed, which can be attributed to OH stretching vibrations of hydroxyl groups, water molecules in the interlayer, and physically adsorbed water,[1] as shown in Scheme 1(a). The hydroxyl stretching band position varies from one trivalent cation to another. This has been related to varying basicity of the hydroxyl group, which is affected by the trivalent cation.[7] The shoulder at 3050 cm^{-1} is related to hydrogen bonding of H_2O to CO_3^{2-} ions in the interlayer space.[16–18] The corresponding HOH bending vibration is located at 1750 cm^{-1},[9] while the 1650 cm^{-1} band is mainly due to HOH bending of physically adsorbed water. The 1750 cm^{-1} band can also be observed in the spectra recorded by Labajos and Rives[19] for Ni–Cr-HTlc, but was not specifically mentioned or assigned. A similar vibration was observed by Kloprogge and Frost[20] in the IR spectrum of takovite (Ni–Al-HTlc) at room temperature. These authors attributed this band to a small amount of water strongly coordinated to cations not incorporated in the hydrotalcite structure. Since no additional phases were observed in our XRD patterns, this assignment is not very likely. Furthermore, IR spectra recorded at higher temperatures indicate that both bands at 1750 and 3050 cm^{-1} follow a similar decreasing trend, suggesting that both vibrations are related to water in the interlayer space. The shoulder at 3050 cm^{-1} is less pronounced in Co–Cr-HTlc than in the other samples, which is directly related with the relatively lower amount of interlayer water in the as-synthesized material.

In the hydroxyl stretching region of the as-synthesized Co–Fe-HTlc sample, two bands (centered at 3500 cm^{-1} with a shoulder at 3420 cm^{-1}) can be identified. In connection to this, two bands (a single band at 872 cm^{-1} and a shoulder at 972 cm^{-1}) appear in the low wavenumber region, assigned to metal–OH deformation. The shoulders at 3420 and 972 cm^{-1} could be due to the OH stretching and deformation of metal–OH bonds separated from the octahedral layers, respectively, although no such species were observed in the XRD pattern of the sample. Nevertheless, the presence of amorphous iron hydroxide carbonate in Co–Fe-HTlc, as was reported by Markov *et al.*,[21] cannot be excluded.

Carbonate vibrations. In the carbonate region of the spectra of the as-synthesized samples, bands are generally located in the range 1390–1414 cm^{-1} (ν_3, asymmetric stretching) and 815–833 cm^{-1} (ν_2, out-of-plane deformation). These bands correspond to the presence of the carbonate anion in a symmetric environment, characterized by a D_{3h} (planar) symmetry. This is usually observed when carbonate groups interact with interlayer water as shown in Scheme 1(a). The presence of a shoulder at 1340–1370 cm^{-1} in the spectra of Co–Al- and Co–Ga-HTlcs at room temperature indicates the presence of a fraction of carbonates in a lower symmetry (C_s or C_{2v}).[18,22] The corresponding C=O vibration should be located at approximately 1570 cm^{-1},[10] but it is difficult to identify in the room temperature spectrum due to overlap with the band around 1400 cm^{-1}. Miyata explained that both monodentate or bidentate carbonate configurations in the interlayer, as illustrated in Scheme 1(b) and (c), give rise to splitting of the carbonate vibrations.[16] *A priori* it cannot be ascertained, from the analysis of the number of bands, which type of carbonate configuration is actually present.[16,23]

The amount of carbonate in a low symmetry environment is more pronounced in the as-synthesized Co–Fe- and Co–Cr-HTlcs, than for the Co–Al- and Co–Ga-HTlcs. For Co–Fe-HTlc (Fig. 6(c)), the ν_3 mode at 1390 cm^{-1} and the presence of a band at 1560 cm^{-1} are indicative of this. The IR spectrum of the as-synthesized Co–Cr-HTlc shows a rather broad band in the carbonate region centered at 1400 cm^{-1}. The high intensity of the shoulders at 1360 cm^{-1} and at about 1500 cm^{-1} (Fig. 6(d)) suggests the presence of a high amount of low-symmetry carbonate in the interlayer space of this sample. An absorption band around 1050 cm^{-1}, assigned to the ν_1 vibrational mode (symmetrical stretching) of the carbonates, was also identified in Co–Fe-HTlc and Co-Cr-HTlc. This vibrational mode is IR inactive for the free symmetric ion,[17,22] and is further evidence of the lower symmetry of the carbonate in the interlayer space in these samples. Fig. 7 shows the increasing trend of the normalized relative ratio of the amount of low-symmetry carbonate and the amount of symmetric carbonate in the spectra of the samples at room temperature (the ratio of the Co–Cr-HTlc sample was set to unity). This correlation shows that the direct interaction of carbonate groups with hydroxyl groups in the brucite-like layers is favoured by the presence of less water in the interlayer space. This is also in excellent agreement with the lower *c* cell parameter calculated for the hydrotalcites (Fig. 1) and the lower weight loss recorded during stage I in the thermogravimetric profile (Fig. 5(a)) upon increasing the cation size.

The situations in Scheme 1(a)–(c) are in agreement with those proposed by Allmann,[24] who stated that the hydroxyl groups of the brucite-like sheets are tied to the CO_3^{2-} groups directly or *via* intermediate H_2O through hydrogen bridges.

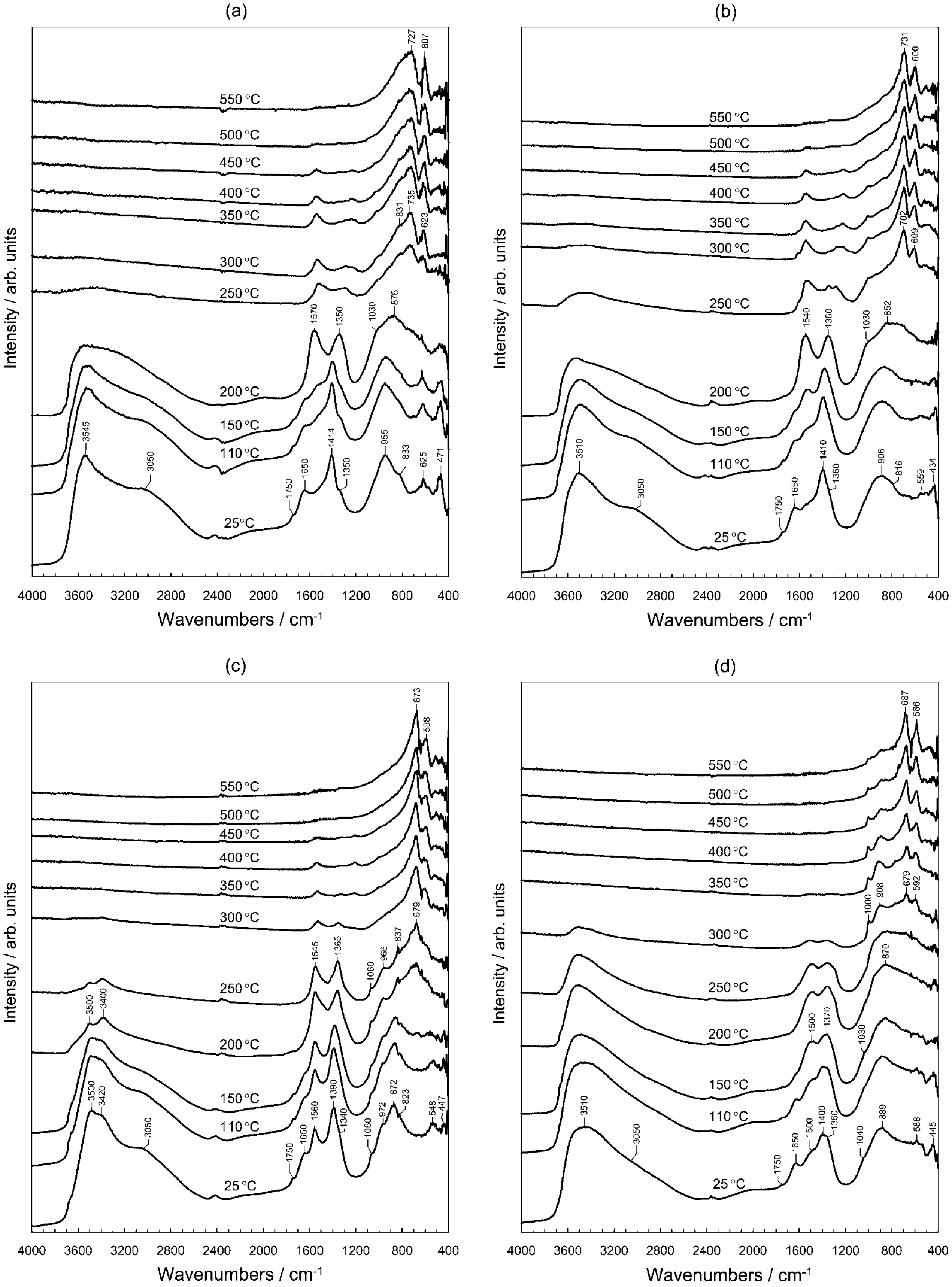

Fig. 6 *In situ* FT-IR spectra for the thermal decomposition of (a) Co–Al-HTlc, (b) Co–Ga-HTlc, (c) Co–Fe-HTlc and (d) Co–Cr-HTlc in air at different temperatures.

Table 1 Positions of the bands (in cm^{-1}) in the IR spectra (Fig. 6), according to the assignments in Scheme 1

Vibration	T/°C	Co–Al-HTlc	Co–Ga-HTlc	Co–Fe-HTlc	Co–Cr-HTlc	Assignment[a]
Water and hydroxyl groups	25	3545	3510	3500	3510	1
		—	—	3420[b]	—	
		1650	1650	1650	1650	
	25	3050	3050	3050	3050	2
		1750	1750	1750	1650	
Carbonates	25	—	—	1560	1500	5
		1414	1410	1390	1400	3
		1350	1360	1340	1360	6
		—	—	1060	1040	$\nu_1(CO_3^{2-})$[c]
		833	816	823	—	$\nu_2(CO_3^{2-})$[d]
	200	1570	1540	1545	1500	5
		1350	1360	1365	1370	6
		1030	1030	1060	1030	$\nu_1(CO_3^{2-})$
	350	1605	1620	—	—	7
		1545	1550	1540	1540	5
		1371	1360	1350	1330	6
		1244	1280	—	—	8
		1220	1230	1210	—	8
		1030	1010	1010	—	$\nu_1(CO_3^{2-})$
Framework	25	—	—	972[b]	—	4
		955	906	872	889	
		625	559	548	588	
		471	434	447	445	
	550	727	731	673	687	9
		607	600	598	586	

[a] See Scheme 1. [b] Assigned to a separate amorphous iron hydroxide carbonate. [c] Symmetrical stretching of the carbonate groups. [d] Out-of-plane deformation of the carbonate groups.

Framework vibrations. In the low-wavenumber region ($<1000\ cm^{-1}$), framework vibrations of the different hydrotalcites can be identified. For Co–Al-HTlc, the band centered at $625\ cm^{-1}$ is assigned to Co–O stretching in the brucite-like sheet, while the band at $471\ cm^{-1}$ belongs to Al–O stretching.[17,20] The band at $955\ cm^{-1}$ is assigned to an Al–OH deformation in the hydrotalcite framework.[25] The varying characteristics of the trivalent cations can also explain the shift in band positions in the framework region, shifting to lower frequencies with increasing atomic mass.

3.4.2. Thermal decomposition. *Dehydration and dehydroxylation.* The first change in the IR spectra of the hydrotalcites occurs upon increasing the temperature from 25 to 110 °C. A decrease in intensity of the bands centered at 3510 and $1650\ cm^{-1}$ is observed, which is related to the loss of physically adsorbed water. In this temperature range, there is also a slight decrease in intensity of the shoulders at 1750 and $3050\ cm^{-1}$ indicating partial removal of interlayer water. These bands have disappeared completely at 200 °C for all the samples. After removal of physically adsorbed water and interlayer water, all remaining IR bands above $3000\ cm^{-1}$ can be assigned to vibrations of OH groups in the octahedral sheets. In transition II at 200–250 °C, substantial dehydroxylation of the brucite-like sheets occurs in the partially decomposed Co-based hydrotalcites. These temperatures are in good agreement with the thermal analysis profiles of these materials shown in Fig. 4. From the intensity of the band around $3500\ cm^{-1}$ in the spectrum at 250 °C, it can be concluded that the hydroxy groups in Co–Cr-HTlc are more stable than in the other samples. This is in agreement with the TGA–DSC result, which shows a relatively high thermal stability of this sample for transition II (see Figs. 4(d) and 5(b)). Complete dehydroxylation in Co–Cr-HTlc requires a temperature of 350 °C, while in the other samples dehydroxylation is complete by 300 °C.

Carbonate rearrangement and decarbonation. Carbonate decomposition shows a similar behaviour for the different samples. Immediately after removal of interlayer water at 200 °C, the splitting of the ν_3 mode of the carbonate in the as-synthesized hydrotalcites (at about $1400\ cm^{-1}$) to bands located at $1340–1370\ cm^{-1}$ and $1500–1570\ cm^{-1}$ becomes more pronounced, especially for the Co–Al and Co–Ga hydrotalcites (see Fig. 6). Additionally, the shoulder at about $1030\ cm^{-1}$ (ν_1 mode, symmetrical stretching) can be clearly identified. This result indicates reorganization of the carbonates to a low-symmetry coordination (C_{2v} or C_v).

The degree of splitting of the carbonate bands observed in the IR spectra at 200 °C is affected by the trivalent cation. The larger the cation, the smaller the splitting of the carbonate bands at this temperature (Fig. 8). This suggests a weaker interaction of the carbonates in the interlayer with the hydroxyl groups (attached mainly to Co). However, at 250 °C the intensities of the carbonate bands show an opposite trend, *i.e.* the stability of the carbonate increases in the series from Al to Cr (Fig. 6(a)–(d)). Apparently not only the strength of the interaction between the hydroxyl groups and the carbonate in the interlayer, but a complex combination of factors, such as the stability of the hydroxides and the layered structure itself, as well as direct interactions of the carbonate with the metal ions, determine how much carbonate is retained in the structure in transition II at 200–250 °C. It should also be mentioned that the trend in carbonate intensity is not in agreement with the increasing weight loss in transition II as a funtion of cation size (Fig. 5(b)). This is explained by the fact that the weight loss contains contributions of both carbonate and hydroxyl group decomposition. This is in agreement with the absence of a clear correlation between the relative amount of spectral contributions of hydroxyl and carbonate groups in the partially decomposed hydrotalcites. The very low intensity of the hydroxyl bands in the Co–Fe-HTlc spectrum at 250 °C (Fig. 6(c)), compared to the carbonate intensity. The hydroxyl/carbonate ratio in *e.g.* Co–Cr-HTlc is much higher (Fig. 6(d)).

The stability of the carbonate configurations in the transition from 250 to 300 °C shows an opposite trend to that from 200 to 250 °C, and decreases as a function of increasing cation size (note the lower intensity of the carbonate bands in the series of spectra at 300 °C). A transition from hydroxylic interactions (Scheme 1(b) and (c)) to coordination to the metal ions (Scheme 1(d) and (e)) is most likely to occur at these temperatures. The complexity of the bands in the carbonate region (see *e.g.* the IR spectrum of Co–Ga-HTlc at 250 °C and

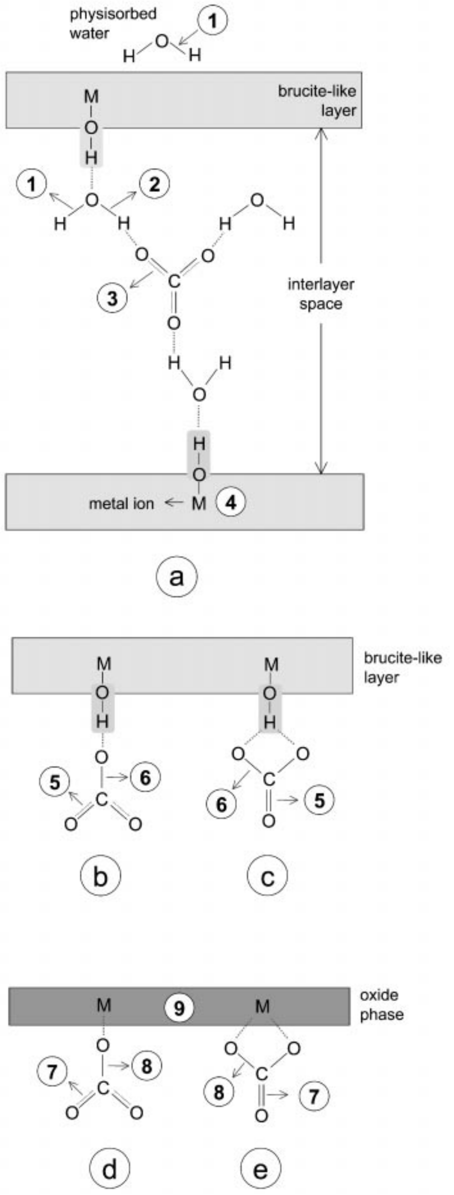

Scheme 1 Assignments during thermal decomposition of Co-based hydrotalcites with different trivalent cations: (a) water, hydroxyl and carbonate vibrations in the as-synthesized hydrotalcite, (b) monodentate or (c) bidentate carbonate configuration interacting with hydroxyl groups in the brucite-like layers after removal of interlayer water, (d) monodentate or (e) bidentate carbonate configuration coordinated to metal ions in the decomposed material (oxidic phase). Assignments 1–8 are listed in Table 1 and discussed in the text.

bands in Table 1) is due to a combination of monodentate and bidentate carbonate configurations. The carbonate stability is now no longer determined by the hydrotalcite structure, but by the interactions with the metal ions in the emerging metal oxide phase, leading to the observed trend. The degree of splitting generally increases with increasing temperature, suggesting an increasing interaction between the metal ions and remaining carbonates in the mixed oxide phase. Oxidation of Cr ions in the corresponding material is likely to affect the low stability of the carbonate in this intermediate compound, which is discussed below. Generally, the carbonate bands completely disappear at 450–500 °C.

Phase transition. In the low-wavenumber region, the lattice vibrations of the as-synthesized Co-based hydrotalcites were observed at 872–955, 559–640 and 434–480. In the spectrum of Co–Al-HTlc at 200 °C, the original band at 955 cm^{-1} (Al–OH deformation) shifts to lower frequencies and develops a weak band around 876 cm^{-1}. The band at 625 cm^{-1} in the as-synthesized material is overlapped by the emerging decomposed phase, while the band at 471 cm^{-1} is less visible, these observations indicate the collapse of the layered double structure and the formation of a spinel-like structure. At 250 °C the doublet in the region 500–700 cm^{-1} of the spectrum of Co–Al-HTlc appears, typical of a normal II–III spinel compound, indicating the loss of lamellar arrangement in the layered structure. In the case of Co–Fe-HTlc the collapse of the layered material occurs at even lower temperature with the appearance of a band related to the final oxidic phase at 679 cm^{-1} in the spectrum at 200 °C. The stability of the layered structure in Co–Cr-HTlc is higher, and the doublet related to the spinel phase is observed at 300 °C. In this sample, two additional bands are identified at 908 and 1000 cm^{-1}, which are attributed to the formation of surface chromates upon decomposition.[7] These chromates are stable, being present even in the spectrum of the sample at 550 °C. The relatively high stability of the Co–Cr-HTlc sample towards collapse and formation of the oxidic phase is related to the high stability of the hydroxy groups in this sample, which only completely decompose at 350 °C (250–300 °C in the other samples). Indeed, dehydroxylation of the brucite-like layers dictates the stability of the hydrotalcite phase.

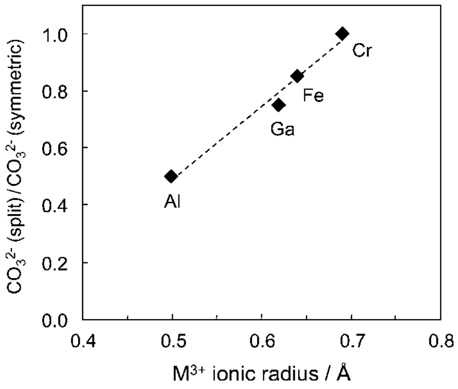

Fig. 7 Correlation between the ratio CO_3^{2-} (split)/CO_3^{2-} (symmetric) in the as-synthesized Co-based hydrotalcites and the ionic radius of the trivalent cation, as derived from Fig. 6 (normalized to unity for Co–Cr-HTlc).

The doublet in the decomposed material below 800 cm^{-1} is indicative of spinel-like mixed oxides. The higher frequency band is due to the AOB_3 and that of lower frequency to the BOB_2 vibrations in the spinel lattice (A denotes tetrahedrally coordinated cations, while B denotes octahedral positions).[26,27] In addition, the bands observed are somewhat shifted with respect to those reported for pure spinel compounds.[28] This result further confirms the presence of a solid solution of cobalt

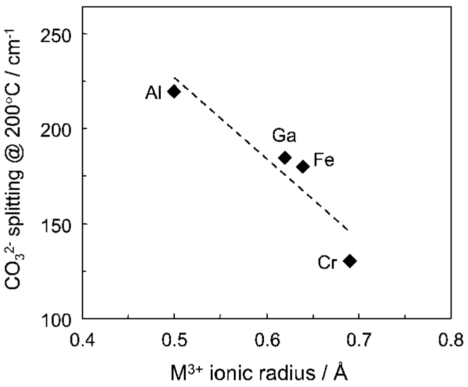

Fig. 8 Correlation between the CO_3^{2-} splitting in the spectra of the decomposed Co-based hydrotalcites at 200 °C and the ionic radius of the trivalent cation, as derived from Fig. 6.

spinels. Additionally the bands are relatively broad, typical for spinel mixed oxides with cationic vacancies.[29]

In all the samples investigated, formation of the oxide phase occurs while some carbonate (and even hydroxyl) groups are still present, indicating the collapse of the layered structure before complete decomposition of these groups. Above 300–350 °C the oxidic phase is formed and the concentration of carbonate is low. Decomposition of these residual carbonate groups causes the weight loss identified as transition III in the TGA–DSC profiles (see Fig. 4).

3.4.3. Evaluation of *in situ* IR results. The different transitions (dehydration, dehydroxylation, carbonate rearrangement and decarbonation, collapse of the layered structure and formation of the oxidic phase) occur in a narrow temperature range for the different samples. Since the spectra were recorded at 50 °C intervals, unfortunately the temperature differences observed in thermogravimetric analysis could not be discriminated by FT-IR.

The relatively low stability of the hydroxyl and carbonate groups in Co-based hydrotalcites was previously observed by thermal analysis and IR emission spectroscopy (IES) for Co–Al-HTlc.[14,25] The transition temperatures observed by IES were in the same range as those observed in our study, although the measurements were performed at a higher heating rate. IES spectroscopy requires high temperatures to achieve good signals and thus the low temperature range (especially for the collapse of the layered structure and the change of symmetry of the carbonates) can not be followed, so limiting its application.[8]

The ability to perform *in situ* measurements using IR spectroscopy is an important aspect of the analysis, since *ex situ* analysis of samples decomposed at different temperatures may lead to rehydroxylation and retrotopotactic crystallization to the originally layered material, which is well-known for the Mg–Al hydrotalcite.[30,31] Additionally, *in situ* IR studies are very suitable to identify possible metastable and/or amorphous intermediate phases during the decomposition process, as we have recently reported with Co–Al hydrotalcite.[32]

4. Conclusions

The following trends in characteristics of Co-based hydrotalcites as a function of the size of the trivalent cation have been determined.

(1) The relative amount of interlayer water in the as-synthesized materials decreases with increasing size of the trivalent cation in the series Al < Ga < Fe < Cr. This is corroborated by:

- A decrease in the *c* parameter as derived from XRD patterns,
- Lower weight loss during the first thermal transition upon thermal decomposition,
- The relative amount of carbonate in high and low symmetry as derived from *in situ* IR spectra.

(2) The crystallinity and crystal size of the as-synthesized samples is affected by the nature of the trivalent cation, being lowest for the Cr-containing sample, but showing no clear trend.

(3) Removal of interlayer water upon thermal decomposition enhances the amount of carbonate in low symmetry, *i.e.* interacting with hydroxyl groups in the brucite-like layer.

(4) The degree of splitting of the ν_3 mode of the carbonate groups at 200 °C is decreased as a function of increasing size of the trivalent cation, suggesting weaker interactions between the carbonate and hydroxyl groups in the octahedral layers of the corresponding dehydrated hydrotalcites.

(5) The thermal stability of the partially decomposed hydrotalcites is dependent on a combination of factors, such as the stability of the hydroxyls.

(6) The interaction of the carbonate with the metal ions in the oxidic phase determines the final temperature for complete carbonate removal.

(7) In general, a higher temperature is required for complete decarbonation than for dehydroxylation. In Co–Cr-HTlc, both dehydroxylation and decarbonation occur simultaneously and are complete at 350 °C.

(8) The *a* parameters of the cobalt mixed oxides show a linear correlation with the size of the trivalent cation in the (cubic) oxide structure.

(9) The crystal size of the mixed oxides is affected by the trivalent cation, but without a clear trend.

Acknowledgements

This research was financially supported by the Council for Chemical Science of the Netherlands Organisation for Scientific Research (CW-NWO). G. M. acknowledges a fellowship granted by the Royal Netherlands Academy of Arts and Sciences. J. B. Taboada is gratefully acknowledged for performing the *in situ* FT-IR experiments.

References

1 F. Cavani, F. Trifirò and A. Vaccari, *Catal. Today.*, 1991, **11**, 173 and references therein.
2 A. Vaccari, *Appl. Clay Sci.*, 1999, **14**, 161 and references therein.
3 H. W. F. Taylor, *Miner. Mag.*, 1973, **39**, 377.
4 R. Allmann, *Acta Crystallogr., Sect. B*, 1968, **24**, 972.
5 N. T. Dung, D. Tichit, B. H. Chiche and B. Coq, *Appl. Catal., A*, 1999, **169**, 179.
6 J. Pérez-Ramírez, G. Mul, J. B. Taboada, F. Kapteijn and J. A. Moulijn, *Proc. 12th International Clay Conference*, 2001, in press.
7 S. Kannan and C. S. Swamy, *J. Mater. Sci.*, 1997, **32**, 1623.
8 J. Pérez-Ramírez, G. Mul, F. Kapteijn and J. A. Moulijn, *Appl. Catal., A*, 2000, **204**, 265.
9 J. Pérez-Ramírez, G. Mul, F. Kapteijn and J. A. Moulijn, *J. Mater. Chem.*, 2001, **11**, 821.
10 J. Pérez-Ramírez, G. Mul and J. A. Moulijn, *Vib. Spectrosc.*, 2001, in press.
11 J. Pérez-Ramírez, J. Overeijnder, F. Kapteijn and J. A. Moulijn, *Appl. Catal., B*, 1999, **23**, 59.
12 S. Kannan and C. S. Swamy, *Catal. Today*, 1999, **53**, 725.
13 S. Miyata, *Clays Clay Miner.*, 1980, **28**, 50.
14 T. Sato, H. Fujita, T. Endo, M. Shimada and A. Tsunashima, *React. Solids*, 1988, **5**, 219.
15 M. A. Ulibarri, J. M. Fernández, F. Labajos and V. Rives, *Chem. Mater.*, 1991, **3**, 626.
16 S. Miyata, *Clays Clay Miner.*, 1995, **23**, 369.
17 M. K. Titulaer, J. B. H. Jansen and J. W. Geus, *Clays Clay Miner.*, 1994, **42**, 249.
18 D. L. Bish and G. W. Brindley, *Am. Mineral.*, 1997, **62**, 458.
19 F. M. Labajos and V. Rives, *Inorg. Chem.*, 1996, **35**, 5313.
20 J. T. Kloprogge and R. L. Frost, *J. Solid State Chem.*, 1999, **146**, 506.
21 L. Markov, V. I. Blaskov, D. Klissurski and S. Nikolov, *J. Mater. Sci.*, 1990, **25**, 3096.
22 F. M. Labajos, V. Rives and M. A. Ulibarri, *Spectrosc. Lett.*, 1991, **24**, 499.
23 N. Nakamoto, *Infrared and Raman Spectra of Inorganic and Coordination Compounds*, John Wiley & Sons, New York, 4th edn., 1986.
24 R. Allmann, *Chimia*, 1970, **24**, 99.
25 J. T. Kloprogge and R. L. Frost, *Appl. Catal., A*, 1999, **184**, 61.
26 B. Gillot, F. Jemmali and A. Rousset, *J. Solid State Chem.*, 1977, **21**, 375.
27 G. Busca, V. Lorenzelli and V. Bolis, *Mater. Chem. Phys.*, 1992, **31**, 221.
28 G. Busca, V. Lorenzelli and V. S. Escribano, *Chem. Mater.*, 1992, **4**, 595.
29 J. Preudhomme and P. Tarte, *Spectrochim. Acta, Part A*, 1971, **27**, 1817.
30 J. Rocha, M. del Arco, V. Rives and M. A. Ulibarri, *J. Mater. Chem.*, 1999, **9**, 2499.
31 F. Millange, R. I. Walton and D. O'Hare, *J. Mater. Chem.*, 2000, **10**, 1713.
32 J. Pérez-Ramírez, G. Mul, F. Kapteijn and J. A. Moulijn, *Mater. Res. Bull.*, 2001, **36**, 1767.